Available online at www.sciencedirect.com
SCIENCE DIRECT®
Icarus ••• (••••) •••–•••
ICARUS
www.elsevier.com/locate/icarus

The peculiar case of the Agnia asteroid family

D. Vokrouhlický [a,*], M. Brož [a], W.F. Bottke [b], D. Nesvorný [b], A. Morbidelli [c]

[a] *Institute of Astronomy, Charles University, V Holešovičkách 2, CZ-18000 Prague 8, Czech Republic*
[b] *Southwest Research Institute, 1050 Walnut St, Suite 400, Boulder, CO 80302, USA*
[c] *Observatoire de la Côte d'Azur, BP 4229, 06304 Nice Cedex 4, France*

Received 14 November 2005; revised 15 March 2006

Abstract

The Agnia asteroid family, a cluster of asteroids located near semimajor axis $a = 2.79$ AU, has experienced significant dynamical evolution over its lifetime. The family, which was likely created by the breakup of a diameter $D \sim 50$ km parent body, is almost entirely contained within the high-order secular resonance z_1. This means that unlike other families, Agnia's full extent in proper eccentricity and inclination is a byproduct of the large-amplitude resonant oscillations produced by this resonance. Using numerical integration methods, we found that the spread in orbital angles observed among Agnia family members would have taken at least 40 Myr to create; this sets a lower limit on the family's age. To determine the upper bound on Agnia's age, we used a Monte Carlo model to track how the small members in the family evolve in semimajor axis by Yarkovsky thermal forces. Our results indicate the family is no more than 140 Myr old, with a best-fit age of 100^{+30}_{-20} Myr. Using two independent methods, we also determined that the $D \sim 5$ km fragments were ejected from the family-forming event at a velocity near 15 m/s. This velocity is consistent with results from numerical hydrocode simulations of asteroid impacts and observations of other similarly sized asteroid families. Finally, we found that 57% of known Agnia fragments were initially prograde rotators. The reason for this limited asymmetry is unknown, though we suspect it is a fluke produced by the stochastic nature of asteroid disruption events.

Keywords: Asteroids, dynamics; Resonances

1. Introduction

Asteroid families, which are clusters of asteroids in proper semimajor axis (a), eccentricity (e), and inclination (i) space produced by asteroid collisions, are among the more intriguing features found in the main asteroid belt. Since their discovery early in the past century (e.g., Hirayama, 1918; historical notes in Bendjoya and Zappalà, 2002), considerable effort has gone toward trying to understand these enigmatic formations. Moreover, as the number of known asteroids has increased, we have become increasingly aware that extended families are "witness plates" to a variety of interesting and poorly understood phenomena.

In this paper, we build on the work described in Vokrouhlický et al. (2006a, 2006b); see also Bottke et al. (2001, 2005a, 2005b) to understand the dynamical structure of asteroid families using modern methods and numerical tools. This means studying (i) how cratering and/or catastrophic disruption events on asteroids produce fragments and (ii) how those fragments evolve over time through collisional and dynamical processes. We focus here on the Agnia family, which resides in the central part of the main asteroid belt at $a \approx 2.79$ AU. This places this family on the periphery of the 5/2 mean motion resonance (MMR) located at $a \approx 2.8$ AU. Other than this resonance, the Agnia family is unaffected by any other MMR of significant strength. On the other hand, we find Agnia exceptional among known asteroid families for how it interacts with the high-order secular resonance z_1 (e.g., Milani and Knežević, 1990, 1992, 1994). Both of these facts will play an important role in story presented below.

* Corresponding author. Fax: +420 2 21 91 25 67.
E-mail address: vokrouhl@mbox.cesnet.cz (D. Vokrouhlický).

0019-1035/$ – see front matter
doi:10.1016/j.icarus.2006.03.002

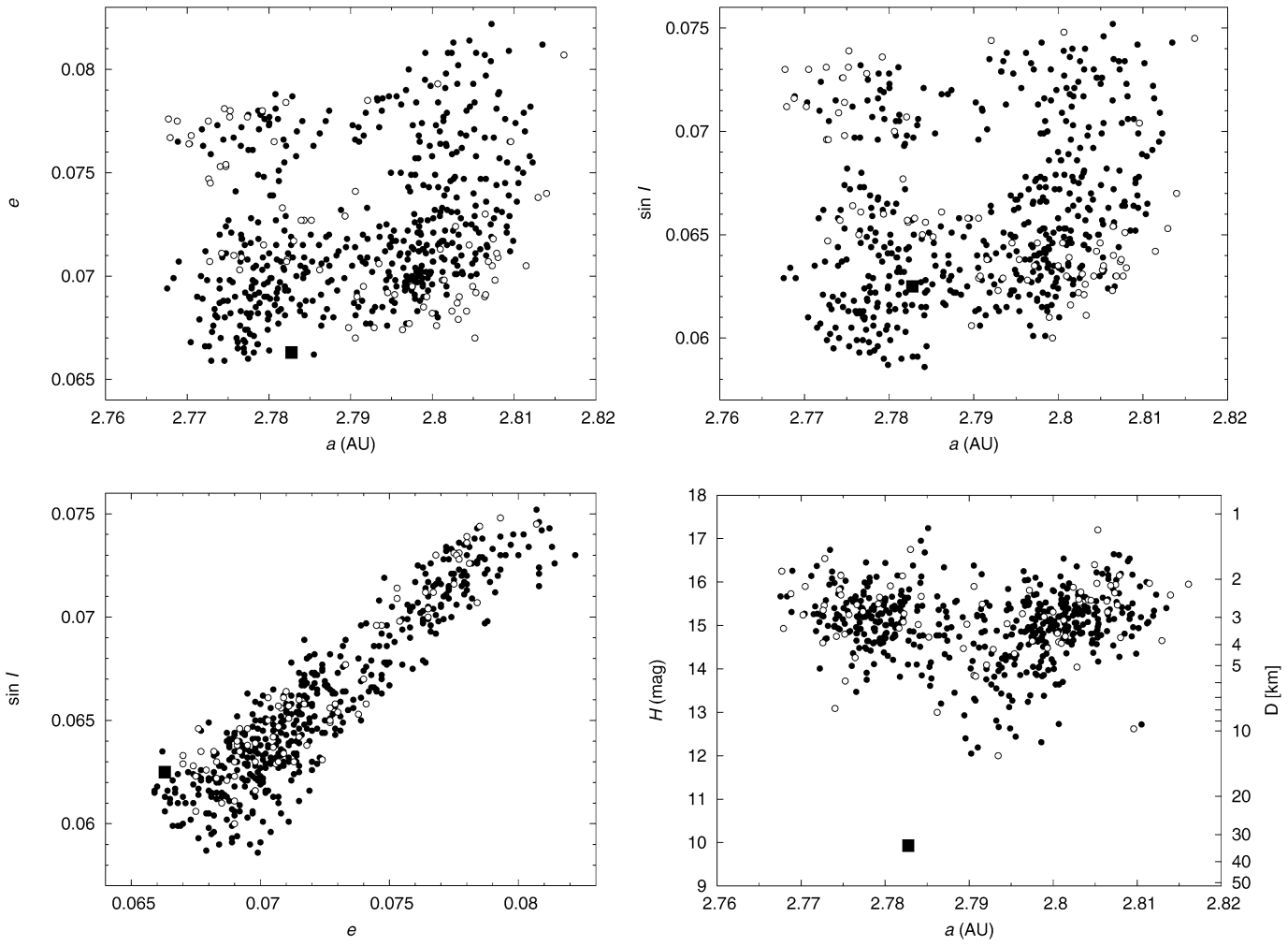

Fig. 1. Projection of the Agnia family, as identified using the HCM method with a cut-off velocity $V_c = 33$ m/s, onto different planes of proper element space parameters: semimajor axis a, eccentricity e, and inclination i. H is the absolute magnitude. The strong correlation of the e and $\sin i$ values (bottom left) indicates presence of a high-order secular resonance z_1 into which most of the family members are immersed (Fig. 4). The center of $H \geqslant 14$ asteroids in semimajor axis, approximately 2.79 AU, is offset from position of the largest Asteroid (847) Agnia (shown as filled square in the bottom right panel). Their difference corresponds to about 30 m/s in terms of along-track velocity. The right ordinate on the bottom right figure indicates the best guess for the size of the members (assumes a geometric albedo $p_V = 0.17$, that of the largest Asteroid (847) Agnia). Filled symbols are Agnia members whose critical angle of the z_1 resonance librates, open symbols are those with the critical angle of the z_1 resonance circulating.

2. Agnia family: basic facts

We start our work by identifying the members of the Agnia family using the hierarchical clustering method (HCM; e.g., Bendjoya and Zappalà, 2002 and references therein). Our code can detect concentrations of asteroids in (a, e, i) space among analytically determined proper elements; more than 170,000 main belt numbered and multi-opposition asteroids exist in the AstDyS database (http://newton.dm.unipi.it/) as of November 2004. We adopt the "standard metric" of Zappalà et al. (1990, 1995) and compute the relative velocity V found between two asteroid orbits. Families are identified when asteroids have V lower than a cut-off velocity value V_c between a neighboring pair of members.

As it is characteristic of compact families, the number of members found by the HCM method increases slowly as a function of V_c until a critical point is reached. At that point, the family members link themselves with the surrounding background population. For the Agnia family, we find this threshold occurs at $V_c = 63$ m/s. Thus a conservative approach for the Agnia family is to keep V_c as low as possible in order to characterize its main features. Hence, our adopted nominal value for the Agnia family is $V_c = 33$ m/s; the interested reader can find data files for this family at different cut-off values on our website http://sirrah.troja.mff.cuni.cz/yarko-site/.

Fig. 1 shows 2-D projections of our nominal Agnia family distribution in proper a, e, i and in absolute magnitude H. Though each of these projections coincides with some interesting feature which will be analyzed below, the most peculiar and singular one is the strong correlation between proper eccentricity e and inclination i values (Fig. 1, left bottom panel). This almost linear relationship is unlikely to be a consequence of the initial ejection velocity field produced by the parent body's disruption, mainly because the inclination and eccentricity dispersions depend on different velocity components. Note that an exception to this rule would be a velocity field in the shape of

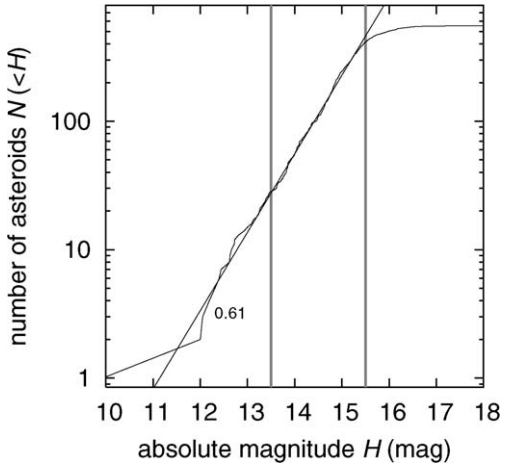

Fig. 2. Cumulative distribution $N(< H)$ of the Agnia members absolute magnitudes H for the nominal identification of the family. Using a power-law approximation $N(< H) \propto 10^{\gamma H}$ in the interval (13.5, 15.5), we find $N(< H)$ is best matched with $\gamma \simeq 0.61$ (straight line).

a highly collimated jet, which has yet to be observed in real families or in numerical simulations of catastrophic disruption events (e.g., Durda et al., 2004). We therefore postulate that the e–i relationship is a consequence of some dynamical effect that shaped the family after it had been formed. Indeed, in the next section we show that the family has been stretched in a specific direction of the (e, i) plane by the influence of high-order secular resonance $z_1 = g + s - g_6 - s_6$.

Fig. 2 shows the cumulative H distribution $N(< H)$ for the Agnia family. It is useful to adopt a power-law approximation $N(< H) \propto 10^{\gamma H}$ to quantitatively express the power law index (or slope) of $N(< H)$ by a single parameter γ. In the range (13.5, 15.5), we find $\gamma \simeq 0.61$. We argue below (see Section 5) that this exponent is unlikely to be a byproduct of collisional evolution; instead, it most likely corresponds to that of the post-breakup distribution of fragments. Note that the accumulation of additional bodies near Agnia makes the size distribution shallower, ultimately reaching a value $\gamma \sim 0.55$. The slope of $N(< H)$ distribution also becomes shallow for $H > 15$; this either stems from observational incompleteness or from an actual change in slope (see, e.g., Morbidelli et al., 2003). If the latter case, the likely cause is collisional evolution between the family members and the background main belt population (Morbidelli et al., 2003; Bottke et al., 2005a, 2005b).

Spectroscopic surveys have determined that (847) Agnia is an S-class asteroid (e.g., Bus and Binzel, 2002a, 2002b; Lazzaro et al., 2004). SMASS II survey also identified (3491) Fridolin, (4051) Hatanaka, (4261) Gekko, (5242) Kenreimonin, (6077) Messner, (7056) Kierkegaard, and (7728) Giblin to be Sq-type asteroids and (1020) Arcadia and (3701) Purkyne to be S-type asteroids. Mothé-Diniz et al. (2005) claim that another five S-type asteroids are associated with the Agnia family, but they lie at $V_c \sim 50$ m/s, which is beyond our nominal identification at $V_c = 33$ m/s. These authors also point out that the dominant spectral classes of the background asteroids in the Agnia vicinity are C or X, very different from family dominating Sq-type asteroids.

Sunshine et al. (2004) claim that Agnia family members, which have a high-calcium pyroxene component in their spectra (and possibly minor amounts of olivine), may have experienced igneous differentiation. A close examination of the large family members, shows that they have very similar spectra. Sunshine et al. (2004) claim this homogeneity may mean that Agnia is a secondary family produced by the breakup of a basaltic fragment from a primary asteroid parent body. Note that the Agnia parent body is only thought to have had a diameter $D \sim 50$ km (Durda et al., 2006, in preparation), which would be consistent with such a scenario. The source and fate of the asteroid that Agnia is derived from is unknown. Bottke et al. (2006) hypothesize that Agnia may be linked to large M-type asteroids like (16) Psyche and (216) Kleopatra, which are generally thought to be iron cores from disrupted differentiated bodies.

IRAS observations of (847) Agnia suggest its albedo is $p_V = 0.172 \pm 0.022$ (Tedesco et al., 2002). This value is consistent with typical S-type asteroids. Little is known about Agnia family members with $H \geqslant 13$ (approximately $D \leqslant 8$ km). In particular, their albedo value has not been determined yet.

We have also attempted to characterize the reflectance spectra of Agnia family members using five color photometry data from the Sloan Digital Sky Survey's (SDSS) (e.g., Ivezić et al., 2001; Jurić et al., 2002). We adopted the same methodology and data analysis as in Nesvorný et al. (2005a). Searching the SDSS database, we found information on 99 Agnia family asteroids. For each of them, we constructed normalized reflectance spectra and computed their principal components PC_1 and PC_2 (see Eq. (1) in Nesvorný et al., 2005a). We then winnowed this down to 26 objects with formal PC_1 and PC_2 errors smaller than 0.1.

Fig. 3 shows these data (filled circles) together with other family members whose PC_1 and PC_2 errors exceed the chosen threshold 0.1 but still fall within the limits of the axes (open circles; there are more asteroids falling even outside). Assuming the bodies have a common mineralogy and hence a parametric relation between PC_1 and PC_2, we identify the Agnia family as a distinct cluster in spectral parameter space in much the same manner as families are identified as clusters in proper element space. From the available high-quality data (filled circles) we can construct a 90% confidence level zone showing family membership (see, e.g., Bertotti et al., 2003, Section 20.5). This is shown with the ellipse in Fig. 3. Two large asteroids, (15675) Goloseevo and (46611) 1993 TH4, fall outside this 90% confidence level threshold, indicating they are only marginally linked to the family. These bodies could be outliers or instead may suggest a possibly larger spectral diversity in the family (compare with Sunshine et al., 2004); in the a–H plane, these two asteroids lie at the border of the family with $a \simeq 2.773$ AU. Note the $PC_1 = 0.3$ spectral slope is the dividing line between the S-complex (for which $PC_1 > 0.3$) and C-complex (for which $PC_1 < 0.3$; e.g., Bus and Binzel, 2002a; Nesvorný et al., 2005a). The Agnia family members fall on both sides of this limit, consistent with more precise spectroscopic data that suggests the family contains numerous asteroids with taxonomic type Sq (Bus and Binzel, 2002a). The mean values

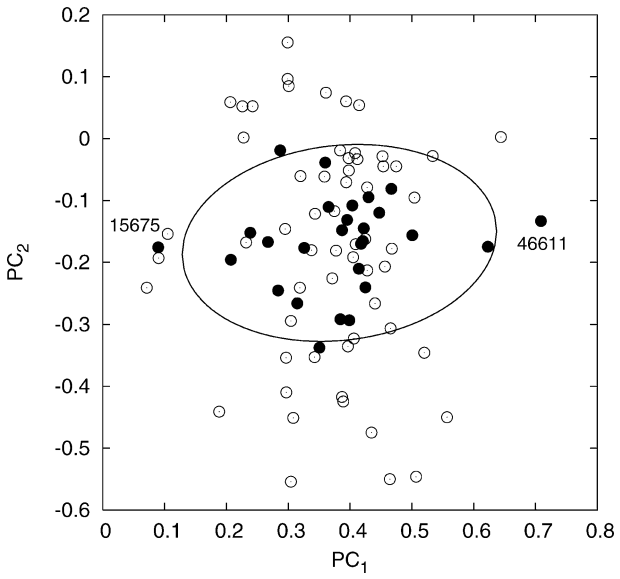

Fig. 3. Principal spectral components PC_1 and PC_2 of the Agnia members from the SDSS five color photometry: (i) full circles are asteroids for which the formal PC_1 and PC_2 errors are smaller than 0.1, (ii) open circles are asteroids for which either of the formal PC_1 and PC_2 errors exceed 0.1. The 90% confidence level region of the family cluster from the good data is shown by the ellipse. Only two members with reliably determined PC_1 and PC_2 values fall outside this limit: (i) (15675) Goloseevo and (ii) (46611) 1993 TH4.

for the spectral components from SDSS data are $PC_1 = 0.38$ and $PC_2 = -0.17$.

3. Agnia family: relation to the z_1 resonance

As described above, the most interesting dynamical aspect of the Agnia family, unique among the known families, is the fact that it is nearly entirely embedded within the high-order secular resonance z_1. In this section, we describe the major features of this peculiar resonance and then discuss our proof that the resonance contains most of the known Agnia family members. The long-term evolution of the Agnia family is described in Section 4.

3.1. z_1 resonance main features in brief

A resonance occurs when a combination of angular variables of the asteroid and planets, called a resonant (critical) angle σ, becomes stationary over long time periods, such that it librates about a fixed center. When the constituting variables do not involve mean anomalies, but only longitudes of node and pericenter of the asteroid and planets, we speak about a secular resonance (e.g., Morbidelli, 2002). This is because σ, as well as the angles on which it depends, is constant in the two-body problem and changes only as a result of planet–asteroid interactions. Thus, their evolution, as well as that of the resonance angle σ, is slow. Consequently, this coherent influence allows even a weak secular resonance to produce significant orbital perturbations over time. Developing a theory describing secular resonances therefore requires to delve into perturbation theory. This can be complicated, particularly when σ comprises more than two secular angles. In that and our case, we are dealing with a high-order secular resonance.

Methods that allow one to systematically analyze high-order secular resonances in the motion of asteroids were pioneered by the work of Milani and Knežević (1990, 1992, 1994). At present, however, no complete analytic or semianalytic theory is yet available for use. Milani and Knežević were principally interested about the degree of instability that high-order secular resonances can produce in the definition of proper orbital elements (e.g., Knežević and Milani, 2000, 2003; Knežević et al., 2002).

However, the high-order secular resonances are important for yet another reason. As demonstrated by several groups (Bottke et al., 2001; Vokrouhlický et al., 2002, 2006a; see also Vokrouhlický and Brož, 2002 and Carruba et al., 2005), they may also serve as pathways for small asteroids drifting in semimajor axis due to the Yarkovsky effect. This process is most clearly identified when it affects the dynamical evolution of asteroids in some well-defined, localized structure such as an asteroid family. For instance, Koronis family asteroids drifting outward (away from the Sun) by the Yarkovsky effect have their proper eccentricities significantly increased when they interact with the $g + 2g_5 - 3g_6$ secular resonance at $a \sim 2.92$ AU (Bottke et al., 2001). A second example includes the small asteroids in the Eos family, which form a stream spreading toward small eccentricity and inclination values along the z_1 resonance (Vokrouhlický et al., 2002, 2006a). Finally, some V-type asteroids appear to have escaped from the Vesta family by migrating along the $z_2 = 2(g - g_6) + s - s_6$ resonance (Carruba et al., 2005).

A fundamental aspect to understanding the Agnia family structure is the $z_1 = g + s - g_6 - s_6$ resonance with resonant angle $\sigma = \varpi + \Omega - \varpi_6 - \Omega_6$ (Milani and Knežević, 1992, 1994). Here ϖ and Ω are the longitude of perihelion and node of the asteroid orbit, while ϖ_6 and Ω_6 are auxiliary angles that change linearly with time and have frequency g_6 and s_6 from planetary theory (e.g., Morbidelli, 2002). The proper frequencies g and s taken from the time series of the ϖ and Ω angles are relevant for the critical angle σ. We thus have $\mathrm{d}\sigma/\mathrm{d}t = g + s - g_6 - s_6$, which is where the nomenclature $z_1 = g + s - g_6 - s_6$ arises (see Milani and Knežević, 1994). It can be easily shown (e.g., Vokrouhlický et al., 2006a) that the conjugated resonant momentum is $\Sigma = G - L = \sqrt{a}(\sqrt{1-e^2} - 1)$, given here in terms of the Delaunay variables L and G or the Keplerian orbital elements a and e. At the simplest level of perturbation theory, the resonant variables are assumed "active," while angles related to the additional dimensions are eliminated from the problem by the averaging principle (e.g., Morbidelli, 2002). Their conjugated momenta are therefore conserved. These are $K_1 = L = \sqrt{a}$ and $K_2 = 2G - H = \sqrt{a(1-e^2)}(2 - \cos i)$. As (Σ, σ) periodically change due to the resonance, e oscillates (note the a is conserved by K_1). Due to conservation of K_2, i is forced to change in a correlated way with e.

Obviously, K_1 and K_2 are conserved only when the sole resonant gravitational perturbations are taken into account. Nonresonant effects will then oscillate with small amplitudes and short periods. More importantly, when non-gravitational effects

such as the Yarkovsky forces are active, they slowly change semimajor axis and allow asteroids to enter, follow, or leave the z_1 resonance. For the sake of the discussion below, we also introduce a modified quantity $K_2' = \sqrt{1-e^2}(2-\cos i)$; that is, by virtue of integrals K_1 and K_2, also conserved in the resonant motion. Below we show by direct numerical integration that it stays approximately constant even when Yarkovsky forces modify the semimajor axis a.

3.2. Agnia members inside the z_1 resonance

Here we show that the orbits of most Agnia members are located inside the z_1 resonance. To do so, we numerically integrated the orbits of all 553 known members of the family for 10 Myr using a SWIFT-RMVS integrator (e.g., Levison and Duncan, 1994). Modifications to this code were made to include the second-order symplectic map from Laskar and Robutel (2001) and to account for Yarkovsky forces (see http://sirrah.troja.mff.cuni.cz/yarko-site/ for details of its implementation, speed and accuracy tests). We computed synthetic proper elements from the code's results in a way compatible with the definitions provided by Knežević and Milani (2000, 2003). This means that we first apply a Fourier filter to the (non-singular) orbital elements in a moving window of $\simeq$0.75 Myr (with steps of 0.1 Myr) to eliminate all periods smaller than some threshold value (in our case, 1.5 kyr). The filtered signal, in the form of mean orbital elements, is then output from the simulation for further checks and passed through a frequency analysis code adapted from Šidlichovský and Nesvorný (1997) to obtain (planetary) forced and free terms in the Fourier representation of orbital elements. The isolated free terms are identified as the proper orbital elements.

The giant planets are included in our simulation with their masses, initial positions and velocities taken from the JPL DE405 ephemeris. We do not include terrestrial planets in the simulation, but we do account for a barycentric correction of the initial conditions; this approximation is justified in the zone of the asteroid belt where Agnia is located (for the problem at hand). The initial orbital elements of the asteroids are taken from the AstOrb database.

Fig. 4 shows the current position of the Agnia members in the plane defined by the critical angle σ of the z_1 resonance and the conjugated frequency $\dot\sigma = g + s - g_6 - s_6$ (that replaces here the conjugated momentum Σ; see originally Milani and Knežević, 1994). In this test we do not include Yarkovsky forces. Our procedure to compute the quantities in Fig. 4 is as follows. The mean orbital elements of asteroids, computed each 0.1 Myr as described above, are Fourier filtered to identify the forced g_6 and s_6 frequencies and their associated phases. The same procedure is followed to get the free frequencies g and s. The frequencies are then plotted on the ordinate and their phases are used to construct the resonant angle σ.

The symbols in Fig. 4, which are given as full or open circles, tell us whether during the 10 Myr timespan the resonant angle σ (i) librates over some restricted interval of values (indicating that the orbit is inside the z_1 resonance) or (ii) circulates and spans all values. Three examples, low-amplitude libration,

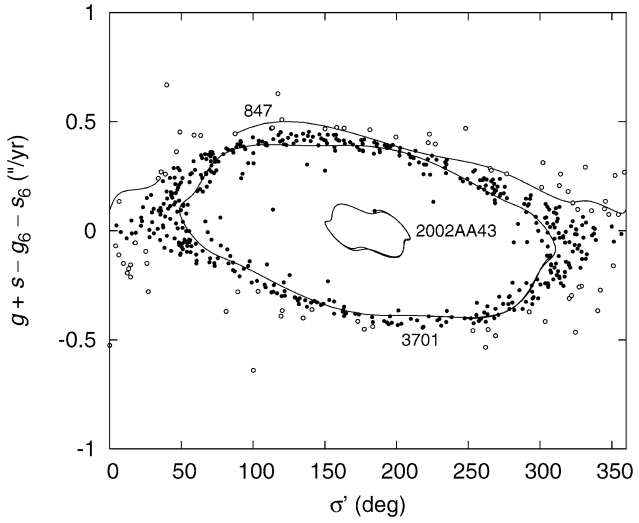

Fig. 4. Agnia family members (symbols) projected onto the plane of critical angle σ of the z_1 resonance vs the associated frequency $\dot\sigma = g + s - g_6 - s_6$. Bulk of the family asteroids reside inside this resonance and close to its separatrix. Filled symbols for librating orbits, open symbols for circulating orbits. The solid lines show evolution paths as determined from 10 Myr numerical integration for three characteristic cases: (i) Asteroid (3701) Purkyne is the most typical evolutionary track in the family (large-amplitude libration), (ii) Asteroid 2002 AA43 is a rare case of small-amplitude libration in the resonance, and (iii) Asteroid (847) Agnia is located right outside the resonance, but very near to its separatrix. Libration period for (3701) Purkyne is about 8 Myr, circulation of (847) Agnia, very close to the separatrix, is even slower. Dispersion of the family members along all values of the resonance angle σ indicates age of the family at least several times the characteristic libration period.

large-amplitude libration (the most typical for the family), and circulation, are shown by the lines and are identified by the asteroid's name. We found that 478 asteroids (thus 86%) are currently located inside the z_1 resonance. We find this to be an exceptional situation; we are not aware of any other asteroid family that is similarly embedded inside a high-order secular resonance. In other families that have been investigated to date (e.g., Eos, Vesta, or Erigone), the secular resonance only affects a small percentage of its members.

What are the implications of this unique feature of the Agnia family? Fig. 5 shows the evolutionary tracks over 10 Myr for our Agnia asteroids, which are now projected onto the plane of synthetic proper elements e and $\sin i$. The effect of this secular resonance forces the proper elements to oscillate in a correlated way, such that $K_2' = \sqrt{1-e^2}(2-\cos i)$ stays constant. It is important to note that the amplitude of these oscillations covers the full extent of the family. This means that the computed values of proper e and i for the Agnia family members only have limited meaning and they change in time along the direction shown in this figure. Because there is a strong sensitivity in this calculation on initial orbital conditions, the relative configuration of the family in the e–i projection, as seen today, does not conserve information about its initial state.

If K_2' is conserved, however, there may be ways to use this information. For the sake of simplicity, let us neglect for the moment the effect of Yarkovsky dispersion of the family (to be analyzed in the next section). We would conclude,

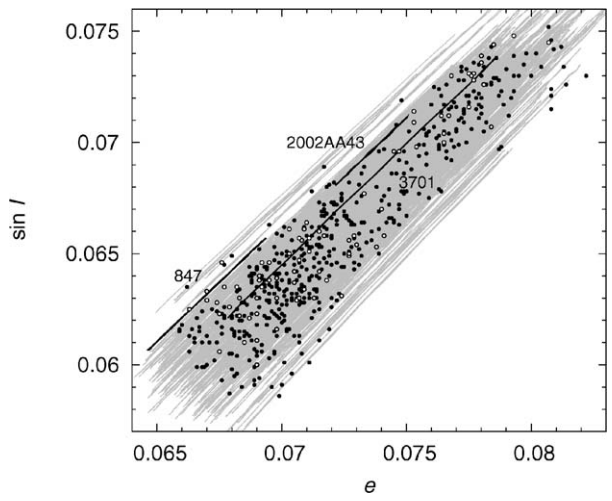

Fig. 5. Agnia family members (symbols) projected onto the plane of proper eccentricity e and sine of inclination $\sin i$. The thick solid lines indicate evolutionary tracks of the three asteroids from Fig. 4. The largest variations correspond to (3701) Purkyne, the large-amplitude libration case. The grey lines are similar 10 Myr evolutionary tracks for all family members. The family is thus stretched along the direction of quasi-integral $K_2' = \sqrt{1-e^2}(2-\cos i)$ and its extension fully determined by the z_1 resonance dynamics.

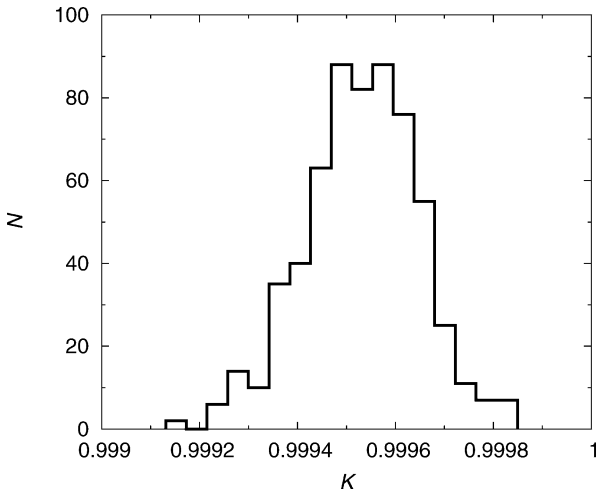

Fig. 6. Distribution of the quasi-integral $K_2' = \sqrt{1-e^2}(2-\cos i)$ values for Agnia members. The characteristic dispersion of $\delta K_2' \simeq \pm 10^{-4}$ in this quantity agrees very well with an initial ejecta dispersion with a typical velocity of $\simeq$15 m/s. This is a value found also by an independent method of semimajor axis dispersion. Unlike the proper orbital elements, the K_2' variable undergoes little dynamical evolution (Fig. 9) and thus in this way the true initial velocity field is imprinted in K_2'-distribution.

in absence of other perturbations (such as weak mean motion resonances; Nesvorný and Morbidelli, 1998; Morbidelli and Nesvorný, 1999), that motion in the z_1 resonance is sufficiently stable to conserve the K_2' value for each asteroid over an extremely long timescale (hundreds of Myr; this value was verified for asteroids in the Eos and Erigone families for both z_1 and z_2 resonances; Vokrouhlický et al., 2006a, 2006b). Thus, the distribution of K_2' values, rather than e and i themselves, stays constant over long time spans, during which it conserves information about the initial state of the family.

Fig. 6 shows the distribution of K_2' for all 553 Agnia members. It is a tight, near Gaussian distribution with a standard deviation (dispersion) of $\sim 1.5 \times 10^{-4}$. In a simple experiment, we tried to transform this information into a characteristic velocity dispersion produced by the breakup of the Agnia parent body (i.e., its initial, post-breakup velocity field). Considering an isotropic velocity field, and assuming that the fragments are dispersed with a Gaussian distribution with a standard deviation V (such as in Petit and Farinella, 1993), our best-fit case for the observed Agnia distribution yields $V \sim 15$ m/s. This low-velocity dispersion value is compatible with results from hydrocode simulations (e.g., Love and Ahrens, 1996; Ryan and Melosh, 1998; Benz and Asphaug, 1999). A similar velocity dispersion was also observed for the Karin family, whose parent body was only slightly smaller than Agnia ($D = 32$ km for Karin vs 50 km for Agnia) (e.g., Nesvorný et al., 2002, 2005a; Durda et al., 2006, in preparation).

4. Agnia family: evolutionary model

Up to this point, we have focused on how the z_1 secular resonance affects proper e and i. Fig. 1, however, shows other interesting features related to the a distribution of Agnia members. It is well known that the semimajor axis values of small asteroids affected by Yarkovsky forces disperse families over time (e.g., Bottke et al., 2002 and references therein). In this section we investigate how this process can be used to constrain the age of the Agnia family.

4.1. Simple numerical model

We first performed a numerical simulation to determine how a synthetic realization of the Agnia family evolves over a timespan of 150 Myr. This final time was not chosen arbitrarily. Rather, it is in agreement with an upper estimate of this family's age from our analysis in Section 4.2. Our primary goal here is to find a lower bound of the family's age based on observations of a nearly uniform distribution of its members along the separatrix of the z_1 resonance (Fig. 4). For that task, we do not include the Yarkovsky forces into our simulation. We also perform a second simulation containing Yarkovsky forces to verify that the K_2' distribution discussed above is conserved (and thus can be used to infer information about the initial state of the family).

First we note that Agnia members are nearly-uniformly distributed along the separatrix of the z_1 resonance (Fig. 4). This implies that the Agnia family cannot be very young. Note that reasonable ejection velocity fields produced by collisional breakup events yield longitudes of perihelion and node dispersed by $\lesssim 10°$. For a typical velocity of $\sim$15 m/s, suggested above from the K_2' dispersion, it would be even less. However, the "uniformity" of Agnia family members in σ does not necessarily require Yarkovsky forces. It can be fully understood from the differential rate of circulation/libration of the angle σ for different asteroids. The time is takes for this to happen can be used to infer a lower limit on the age of the Agnia family.

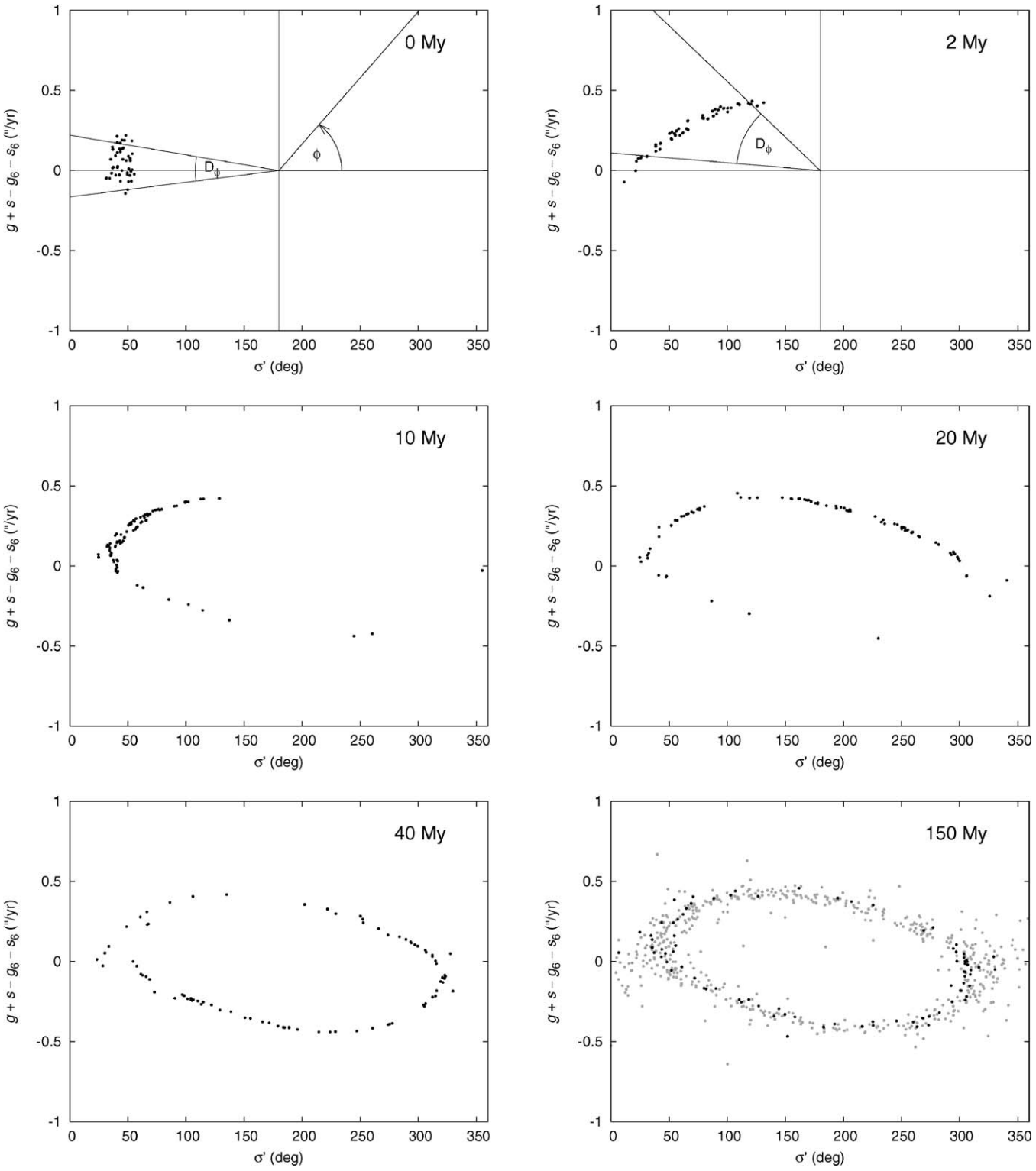

Fig. 7. Snapshots of the numerically integrated evolution of the Agnia family projected onto the z_1 resonance variables: initial state of 92 tightly clustered bodies (top left), 2 Myr (top right), 10 Myr (middle left), 20 Myr (middle right), 40 Myr (bottom left), 150 Myr (bottom right). After about 40 Myr the clump becomes entirely dispersed near separatrix of the resonance with no memory of the initial state; the last frame (at 150 Myr) shows both the numerically integrated particles (bold symbols) and the true Agnia family (light symbols). The auxiliary angle ϕ, whose origin and sense is shown on the top left panel, is used to better describe dispersion of the clump (see Fig. 8 and the text). An animation of our complete simulation can be found at http://sirrah.troja.mff.cuni.cz/yarko-site/.

For this purpose, we conducted the following numerical experiment. We started with a synthetic Agnia family as a tightly compact cluster in a, e, i, and σ. Within the z_1 resonance, this fake family is initially a compact cloud as shown in the first panel of Fig. 7. To better define the circulation time, our fake family is composed of a subgroup of 23 observed Agnia fam-

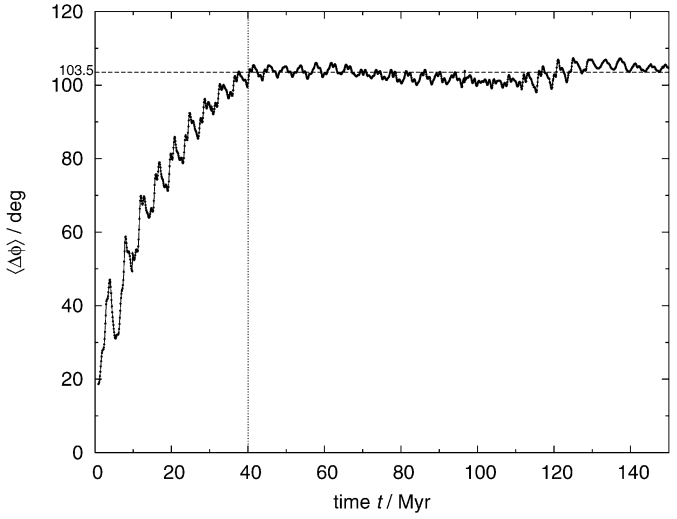

Fig. 8. Temporal evolution of D_ϕ from Eq. (1) issued to measure dispersion of the synthetic Agnia family along the separatrix of the z_1 resonance. Initially, the family starts very compact, but after ≃40 Myr D_ϕ attains the currently observed value of ≃103° with no further evolution. This value corresponds to a uniformly distributed sample along the separatrix. The oscillation, especially near the initial epoch, are due to slower change in ϕ near the unstable stationary foci of the z_1 resonance (i.e., near $\sigma = 0°$ and 360°).

ily members and 3 sets of "clones" produced by adding small values to the eccentricities and inclinations of the real objects. Thus, we integrated 92 bodies in all.

Fig. 7 shows the evolution of our synthetic family as tracked in the space of z_1-resonance variables $(\sigma, \dot\sigma)$. We note that the initially tight cluster of objects spreads in time. After ∼40 Myr, it becomes uniformly dispersed along the separatrix of the z_1 resonance. To quantitatively describe the distribution of bodies along the z_1 separatrix, we define an auxiliary polar angle ϕ in the $(\sigma, \dot\sigma)$-plane (Fig. 7). This means that we have compromised in scaling the two axes; we use a scaling that maps a (0°, 360°) interval of σ and $(-1, 1)$ arcsec/yr interval in $\dot\sigma = g + s - g_6 - s_6$ into common intervals $(-1, 1)$. At each timestep of our numerical simulation, we compute a dispersion D_ϕ in the polar angle ϕ defined as

$$D_\phi^2 = \frac{1}{N(N-1)} \sum_{i \neq j} (\phi_i - \phi_j)^2, \qquad (1)$$

where $N = 92$ is the number of integrated bodies and ϕ_i is the polar angle of the ith body ($i = 1, \ldots, N$). Since we start with a compact cluster, D_ϕ is initially small (∼7°) but grows with time due to differential libration of the bodies in the resonance (Fig. 8). The wavy pattern in the time evolution of D_ϕ is due to the different libration speeds of bodies near the unstable loci $\sigma \sim 0°$ or 360° and the one near $\sigma \sim 180°$. We note that after ∼40 Myr, the value of D_ϕ saturates at ∼103.5°. This can easily be shown to correspond to a uniform distribution of bodies along a circle, and the value also holds for currently observed Agnia members. This result confirms that the Agnia family is more than 40 Myr old.

Fig. 9 shows a time dependence of similarly defined dispersion D_e of proper eccentricity and dispersion $D_{\sin i}$ of the sine of the proper inclination. They show a similar pattern to that of D_ϕ with higher-amplitude oscillations. Another outstanding feature of the Agnia family is its depletion in the center of the proper element cloud (Fig. 1). The same pattern can be found in the individual distributions of proper a, e, i. We deal with the case of proper a in next section, while here we observe that the depletion in the mid e- and i-distributions comes naturally in our simulation from asteroids that spend more time near the unstable loci at $\sigma \sim 0°$ and 360° (similarly to the well-known pendulum case).

Next, we repeat our numerical simulation above with Yarkovsky forces included. The goal here is to verify the near-conservation of the K_2' variable even in this generalized case. We start with the same initial data as before. The sizes of the our integrated bodies (23 asteroids and clones) are computed from their H values and a geometric albedo of 0.17. Most of these bodies are $3 < D < 8$ km in diameter (Fig. 1, bottom left panel). We assign them low-surface conductivity values of $K = 0.002$ W/m/K, surface and bulk densities of 1.5 and 2.5 g/cm^3 and specific heat capacity 680 J/kg/K (values expected for regolith-covered multi-kilometer main belt asteroids). Rotation periods are given a Gaussian distribution peaked at 6 h, but values smaller than 3 h and larger than 12 h are excluded. Spin axis obliquities are set to represent a random distribution of spin axes in space. Because these initial data are unconstrained, we do not attempt in this simulation to fit the observed a distribution among the Agnia family members. This will be approached in the next section using a Monte Carlo technique.

All our previous results are similar to the new runs, except now 4 bodies out of 92 managed to escape from the resonance due to Yarkovsky drift. We focus our attention on the behavior of the dispersion D_K of the K_2' quantity defined above (shown as a bold lower curve in Fig. 9). Interestingly, D_K is nearly constant over the entire integration timespan of 150 Myr; major perturbations only occur when some of the bodies leave the z_1 resonance. This result is important because it confirms that we can use the currently observed K_2' distribution to infer quantitative information about the initial velocity field (Section 3.2 and Fig. 6).

4.2. Semimajor axis distribution fitted

We are now finally in a position to explore the semimajor axis evolution of Agnia family members. We find that the observed a distribution is characterized by those small members that have achieved extreme a values (Fig. 1). Our method here closely follows the work of Vokrouhlický et al. (2006b), who showed that such a skewed distribution is a consequence of the Yarkovsky–O'Keefe–Radzievskii–Paddack (YORP) effect. Objects have their spin axes evolve to alignments perpendicular to the orbital plane, which in turn accelerates the Yarkovsky migration of asteroids and depletes the family center. In what follows, we apply the method of Vokrouhlický et al. (2006b) to the Agnia case.

Consider family members projected onto the plane of proper semimajor axis a and absolute magnitude H. By choosing a center a_c of the family, typically (but not necessarily) close

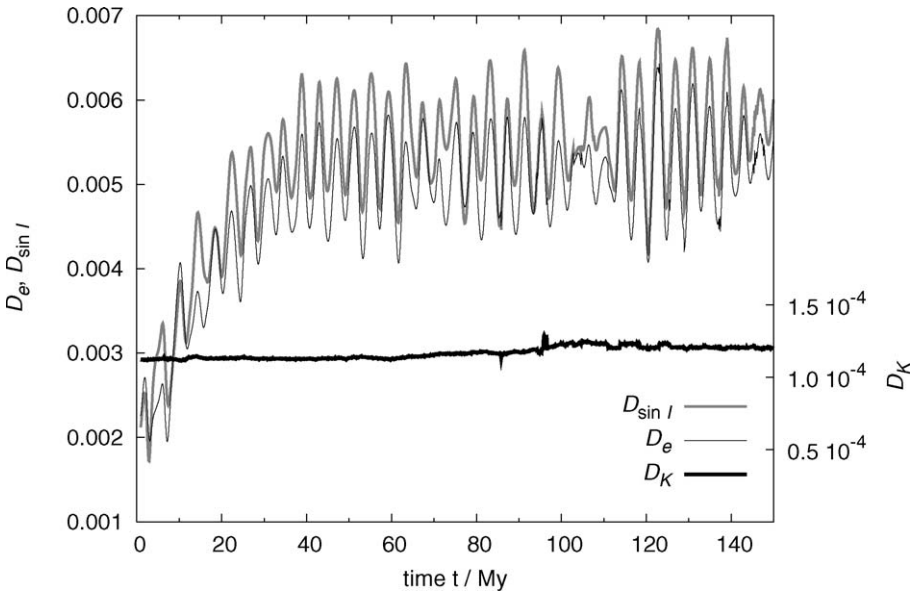

Fig. 9. Temporal evolution of D_e and $D_{\sin i}$ (left ordinate) which undergo both: (i) long-term increase with saturation at $\simeq$40 Myr (compare with D_ϕ in Fig. 8), and (ii) large oscillations with a period of near-separatrix libration. The right ordinate and bold lower curve shows temporal evolution of D_K, dispersion of the K_2' variable, now determined in the simulation that contains the Yarkovsky forces. D_K is quasi-constant with only very small change due to few particles that escaped from the z_1 resonance.

to the largest body, we assign a parameter C to each asteroid according to $0.2H = \log(\Delta a/C)$, with $\Delta a = a - a_c$. We characterize the distribution of these family members using a one-dimensional array $N_{\rm obs}(C)$ that indicates the number of asteroids occupying a bin $(C, C + \Delta C)$ for some suitable value of ΔC. An effort is then made to match the observed distribution $N_{\rm obs}(C)$ with a model prediction of $N(C)$ objects in the $(C, C + \Delta C)$ bin. To that end, Vokrouhlický et al. (2006b) search to minimize a "target (χ^2-like) function" (see also Press et al., 2001)

$$\Psi_{\Delta C} = \sum_{\Delta C} \frac{[N(C) - N_{\rm obs}(C)]^2}{N_{\rm obs}(C)} \qquad (2)$$

by varying the free parameters in the model. Note the occurrence of $N_{\rm obs}(C)$ in the denominator of (2) which may be formally interpreted as assigning $\sqrt{N_{\rm obs}(C)}$ errors to the observed number of asteroids in the appropriate bin. Admissible solutions are characterized by $\Psi_{\Delta C}$ of the order equal to the number of used bins in C, while solutions giving much larger $\Psi_{\Delta C}$ are incompatible with the observed family. We use the incomplete gamma function $Q(M, \Psi^\star_{\Delta C})$ as a goodness-of-fit parameter (see, e.g., Press et al., 2001), where M is the number of ΔC-bins minus three (number of free parameters) and $\Psi^\star_{\Delta C}$ is the minimum value of the target function (2). Since our best solution yields a high-quality fit ($Q = 0.97$), we simplify the parameter-error analysis by deriving them from the level curve of $\Psi_{\Delta C} = M + 3$, i.e., level curve of the target function equal to the number of ΔC-bins ("observations"). Solution of this $\Psi_{\Delta C}$ level-curve correspond to $Q \sim 0.2$–0.3 according to number of degrees.

As far as our theoretical model is concerned, we use the same Monte Carlo approach as described in Vokrouhlický et al. (2006b). Namely, we start with an initial, post-breakup a distribution for the family asteroids using a simple model with an isotropic velocity field. Fragments of a characteristic size, 5 km in our case, are assumed to be dispersed with a Gaussian distribution of velocity components having a standard deviation value of V (fragments of different sizes D are assumed dispersed with a velocity inversely proportional to D). V is one of the free parameters to be solved for in minimization of $\Psi_{\Delta C}$. After defining the initial conditions, each asteroid evolves in a due to Yarkovsky forces over a time interval defined as the age of the family T. The strength of the Yarkovsky forces depends on some assumed thermal parameters and also on the spin state of the asteroid.[1] The latter quantity is folded into a dependence on the obliquity ϵ and rotation period P. While these parameters are set at the initial time, they are assumed to evolve over the long-term due to the YORP effect (Rubincam, 2000; Vokrouhlický and Čapek, 2002). We use a characteristic strength of the YORP effect computed by Čapek and Vokrouhlický (2004) for a large sample of objects with different random shapes and surface conductivities. The uncertainties in modeling of the YORP effect are adjusted by including a third free parameter $c_{\rm YORP}$ that linearly multiplies the YORP influence on ϵ and P. Finally, we run numerous simulations over a matrix of different values for the free parameters $(T, V, c_{\rm YORP})$. Then, for each run, we compute the target function $\Psi_{\Delta C}$ and search for parameters that lead to its minimum value.

Fig. 10 (symbols in the upper left part) shows the distribution of $N_{\rm obs}(C)$ values for the Agnia family and $\Delta C = 1.5 \times 10^{-6}$ AU. The computed distribution was derived as a

[1] We use a linearized approximation by Vokrouhlický (1998, 1999) and Vokrouhlický and Farinella (1999) to obtain the diurnal and seasonal components of the semimajor axis secular change $\mathrm{d}a/\mathrm{d}t$.

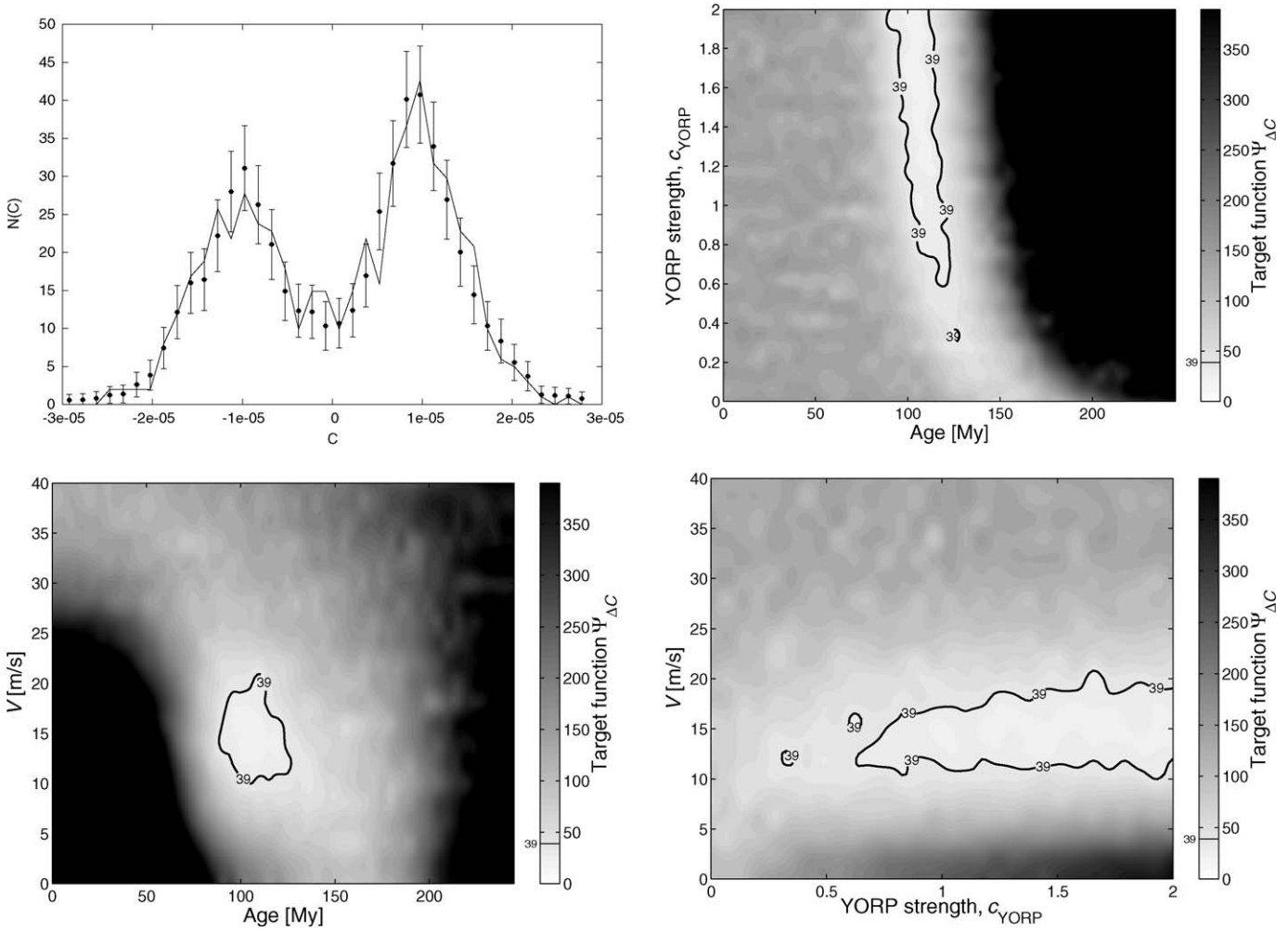

Fig. 10. Results of our simulation for the Agnia family with mean albedo $p_V = 0.17$ and surface thermal conductivity randomly spanning $K = 0.001$–0.01 W/m/K. The best-fit solution $N(C)$ (solid line in the top left panel) is shown with the observed data $N_{obs}(C)$. These were obtained by $(C, C + \Delta C)$ binning with $\Delta C = 1.5 \times 10^{-6}$ AU and a_c uniformly averaged in the range $(2.788, 2.792)$ AU. We assign a formal error-bars of $\sqrt{N_{obs}(C)}$ to $N_{obs}(C)$. Note a slight asymmetry of the data about $C = 0$ with significant maxima at $C = \pm 10^{-5}$ AU. The other three panels show projection of the best value of the target function $\Psi_{\Delta C}$ for various pairs of the solved-for parameters: (i) age T vs YORP strength parameter c_{YORP}, (ii) age T vs characteristic velocity V of initial ejection of $D = 5$ km fragments, and (iii) c_{YORP} vs V. Formal 1σ contour, defined by $\Psi_{\Delta C} = 39$ (number of bins in C; see the text), is shown in bold; contours for other values of the target function are shown using shading and the value-bar on the right.

mean over central values a_c in $(2.788, 2.792)$ AU (i.e., near the center of small members in the family). If we were using only a single a_c value from this interval, some of the bin occupancies would show random fluctuations that would affect our fit. We eliminated this potential problem by computing the $N_{obs}(C)$ distribution using an average over results for which a_c spans a small interval near the unknown center of the family. The concentration of small Agnia members toward extreme values of a is seen in $N_{obs}(C)$ as two significant maxima that are offset from the center at $C \sim \pm 10^{-5}$ AU. They are slightly asymmetric, showing that there are more Agnia asteroids with $a \geqslant a_c$ (see also Fig. 1).

The largest asteroid, (847) Agnia, is offset by $\simeq 0.005$ AU from the center of the smaller members in the family (Fig. 1). Though unusual, this feature may mean the fragments were ejected with an anisotropic velocity field (see, e.g., examples in Marzari et al., 1996). The a displacement described above corresponds to ~ 30 m/s in the transverse velocity component, comparable with the characteristic velocity dispersion of smaller family members that are discussed below.

Fig. 10 shows results from our simulation where we considered the surface conductivity K of Agnia members as a random variable in the range 0.001–0.01 W/m/K. More precisely, we distribute the quantity $\log K$ uniformly in the interval $(-3, -2)$. We assumed surface and bulk densities of 1.7 and 2.5 g/cm^3 and specific thermal heat capacity $C = 680$ J/kg/K. In addition to the three solved-for parameters (T, V, c_{YORP}), we introduced a fourth parameter ξ which yields the fraction of initially prograde rotating asteroids. Each set of matrix runs assumed a different value of ξ. The goal was to better describe the asymmetry of the $N_{obs}(C)$ distribution. Fig. 10 suggests $\xi \geqslant 0.5$. Thus, we tested values in the interval $(0.5, 0.75)$.

The minimum value of the target function $\Psi_{\Delta C}$ obtained with our model was 22, significantly less than the number of C-bins ($M = 39$). For this reason, we consider our result statistically sound; this is also confirmed by the quality-factor

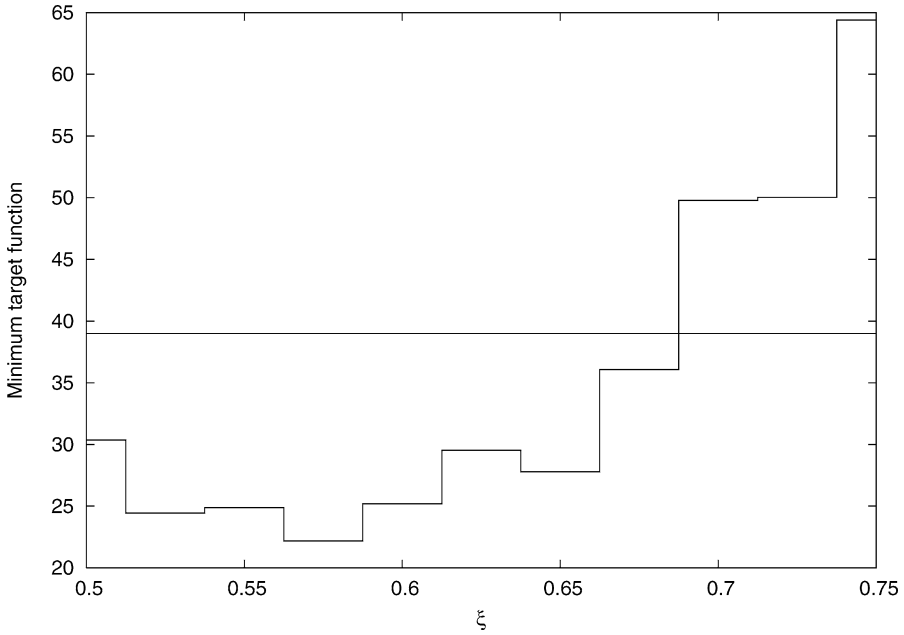

Fig. 11. Minimum values of the target function $\Psi^{\star}_{\Delta C}$ for different values of the asymmetry parameter ξ characterizing initial proportion of the prograde vs retrograde rotating fragments. The best-fit solution slightly prefers more prograde rotators among initial collision ejecta (57% vs 43%). Statistically admissible solutions are, however, obtained also for symmetric partition of prograde/retrograde rotators.

value $Q = 0.97$. If, for simplicity, we thus used the threshold $\Psi_{\Delta C} = 39$ to define the standard error of the solved-for parameters, our best-fit solution would read: $T = 100^{+30}_{-20}$ Myr, $V = 16^{+4}_{-6}$ m/s, and $c_{\mathrm{YORP}} = 0.9^{+1.1}_{-0.3}$. These values correspond to $\xi = 0.57$, which may indicate a slight asymmetry between the number of prograde and retrograde rotating asteroids produced by the initial breakup of the family. Fig. 11 shows how the minimum-acquired $\Psi^{\star}_{\Delta C}$ depends on different choices of ξ, indicating even an equal partition ($\xi = 0.5$) could still offer a statistically reasonable though less satisfying solution. Conversely, ξ must be smaller than 0.68, a value that would lead to an unjustified asymmetry between the initially prograde and retrograde rotators.

Interestingly, our best-fit value of $\xi = 0.57$ is similar to that found by Nesvorný and Bottke (2004) for the members of the young Karin cluster. The source of this asymmetry is unknown. One possibility is that there is something intrinsic in the breakup process that produces more prograde than retrograde objects (e.g., La Spina et al., 2005). A second possibility is that the value of ξ produced in different breakup events follows a Gaussian distribution centered around $\xi = 0.5$. If true, the similarities between Agnia and Karin families may be a statistical fluke. Finally, a third possibility is that immediately after a family-forming event, fragments take some time to generate regolith. In the interim, their higher K values, which may be closer to bare rock than a regolith-covered surface, may allow the seasonal Yarkovsky effect to dominate the diurnal variant, such that all asteroids drift inward. This effect would create an offset in the family's semimajor axis distribution that would be skewed toward smaller a values. Eventually, the family asteroids would develop regolith and return to a state where their migration was dominated by the diurnal Yarkovsky effect (which allows asteroids to evolve both inward toward and outward away from the Sun). Of these three possibilities, we can rule out the last one for Agnia because it appears to have more members further from the Sun than closer to the Sun.

According to Vokrouhlický et al. (2006b) the best-fit value of T roughly scales with $\sqrt{p_{\mathrm{V}}}$, such that a smaller mean albedo value for Agnia family members (in the multi-kilometer range) would make the family older. An albedo value smaller than ~0.1, however, is unlikely. For this reason, we consider the upper age of the Agnia family to be ~140 Myr. If small family members have higher albedo values than predicted here (e.g., Tedesco et al., 2002), the Agnia family's age might be smaller than 100 Myr, with the lower bound set at 40 Myr (Section 4.1). We also find it interesting that the best-fit value of the characteristic dispersion velocity V of $D = 5$ km Agnia members is compatible with our estimate from an analysis of the K'_2 function distribution (Fig. 6). As in Vokrouhlický et al. (2006b) the strength of the YORP effect is loosely constrained with only the no-YORP solution ($c_{\mathrm{YORP}} = 0$) statistically excluded.

5. Conclusions

The unique relation of the Agnia asteroid family to the high-order resonance z_1 allows a deeper insight into its evolution and initial state than is possible with other families of comparable size and age. We have shown this by placing independent, and consistent, constraints on the age of this family. We have also derived a characteristic velocity for multi-kilometer family members that is consistent with estimates from other small families.

Interestingly, Bottke et al. (2005a, 2005b) find that the mean disruption lifetime of a $D \sim 2$ km asteroid in the main belt is ~700 Myr. If this estimate is true, most observed Agnia members are original fragments that have not yet experienced sec-

ondary fragmentations. The Agnia family, together with other even younger families (Nesvorný et al., 2002, 2003), might be thus a good laboratory to study outcome of the collisional fragmentation of large main belt asteroids (see, e.g., Nesvorný et al., 2005b).

We note that a relatively young age found for this family is in agreement with the dominant Sq spectral type of its members, and a related small mean value of PC_1 found from the SDSS data. Jedicke et al. (2004) and Nesvorný et al. (2005a) interpret both in the frame of a space weathering scenario.

A preliminary analysis indicates that the Agnia family is unlikely to be a significant contributor to the dust and micrometeorite population produced by main belt collisions. Using the code described in Bottke et al. (2005c), we examined dust population from the present-day Agnia family. Our results suggest that Agnia-derived dust is likely to be 2–3 orders of magnitude smaller than that produced by the background main belt population. This is because the family is both small (parent body $D \sim 50$ km) and modestly old ($\sim$100 Myr); the combination means that its dust/micrometeorite population has likely reached quasi-collisional equilibrium with the background population. Thus, unless the tight (a, e, i) clustering of the Agnia family can overcome its putative low dust production rate, the Agnia family is unlikely to be a source of some of the weak dust bands proposed by Sykes (1988).

Finding smaller asteroid families in the main belt, studying their structure, and linking this analysis to the physics of collisional processes, origin of interplanetary dust and meteorite science is an interesting long-term project. Our study of the Agnia family is a piece of mosaic indicating our current ability to fulfill this task.

Acknowledgments

This work has been supported by the Grant Agency of the Czech Republic (Grant 205/05/2737) and NASA's Planetary Geology & Geophysics program (W.F.B. and D.N.). We thank Z. Knežević and G.B. Valsecchi for suggestions that helped to improve the original version of this paper.

References

Bendjoya, P., Zappalà, V., 2002. Asteroid family identification. In: Bottke, W.F., Cellino, P., Paolicchi, A., Binzel, R.P. (Eds.), Asteroids III. Univ. of Arizona Press, Tucson, pp. 613–618.

Benz, W., Asphaug, E., 1999. Catastrophic disruptions revisited. Icarus 142, 5–20.

Bertotti, B., Farinella, P., Vokrouhlický, D., 2003. Physics of the Solar System. Kluwer Academic, Dordrecht.

Bottke, W.F., Vokrouhlický, D., Brož, M., Nesvorný, D., Morbidelli, A., 2001. Dynamical spreading of asteroid families via the Yarkovsky effect: The Koronis family and beyond. Science 294, 1693–1695.

Bottke, W.F., Vokrouhlický, D., Rubincam, D.P., Brož, M., 2002. Dynamical evolution of asteroids and meteoroids using the Yarkovsky effect. In: Bottke, W.F., Cellino, A., Paolicchi, P., Binzel, R.P. (Eds.), Asteroids III. Univ. of Arizona Press, Tucson, pp. 395–408.

Bottke, W.F., Durda, D.D., Nesvorný, D., Jedicke, R., Morbidelli, A., Vokrouhlický, D., Levison, H.F., 2005a. The fossilized size distribution of the main asteroid belt. Icarus 175, 111–140.

Bottke, W.F., Durda, D.D., Nesvorný, D., Jedicke, R., Morbidelli, A., Vokrouhlický, D., Levison, H.F., 2005b. Linking the collisional history of the main asteroid belt to its dynamical excitation and depletion. Icarus 179, 63–94.

Bottke, W.F., Durda, D.D., Nesvorný, D., Jedicke, R., Morbidelli, A., Vokrouhlický, D., Levison, H.F., 2005c. The origin and evolution of stony meteorites. In: Knežević, Z., Milani, A. (Eds.), Dynamics of Populations of Planetary Systems. Cambridge Univ. Press, Cambridge, pp. 357–374.

Bottke, W.F., Nesvorný, D., Grimm, R.E., Morbidelli, A., O'Brien, D.P., 2006. Iron meteorites are remnants of planetesimals formed in the terrestrial planet region. Nature 439, 821–824.

Bus, S.J., Binzel, R.P., 2002a. Phase II of the small main-belt asteroid spectroscopic survey. The observations. Icarus 158, 106–145.

Bus, S.J., Binzel, R.P., 2002b. Phase II of the small main-belt asteroid spectroscopic survey. A feature-based taxonomy. Icarus 158, 146–177.

Čapek, D., Vokrouhlický, D., 2004. The YORP effect with finite thermal conductivity. Icarus 172, 526–536.

Carruba, V., Ferraz-Mello, S., Michtchenko, T.A., Roig, F., Nesvorný, D., 2005. On the V-type asteroids outside the Vesta family. I. Interplay of non-linear secular resonances and the Yarkovsky effect. The cases of 956 Elisa and 809 Lundia. Astron. Astrophys. 441, 819–830.

Durda, D.D., Bottke, W.F., Enke, B.L., Merline, W.J., Asphaug, E., Richardson, D.C., Leinhardt, Z.M., 2004. The formation of asteroid satellites in large impacts: Results from numerical simulations. Icarus 170, 243–257.

Hirayama, K., 1918. Groups of asteroids probably of common origin. Astron. J. 31, 185–188.

Ivezić, Z., and 32 colleagues, 2001. Solar System objects observed in the Sloan Digital Sky Survey commissioning data. Astron. J. 122, 2749–2784.

Jedicke, R., Nesvorný, D., Whiteley, R., Ivezić, Z., Jurić, M., 2004. An age–color relationship for main-belt S-complex asteroids. Nature 429, 275–277.

Jurić, M., and 12 colleagues, 2002. Comparison of positions and magnitudes of asteroids observed in the Sloan Digital Sky Survey with those predicted for known asteroids. Astron. J. 124, 1776–1787.

Knežević, Z., Milani, A., 2000. Synthetic proper elements for outer main belt asteroids. Celest. Mech. Dynam. Astron. 78, 17–46.

Knežević, Z., Milani, A., 2003. Proper element catalogs and asteroid families. Astron. Astrophys. 403, 1165–1173.

Knežević, Z., Lemaître, A., Milani, A., 2002. The determination of asteroid proper elements. In: Bottke, W.F., Cellino, A., Paolicchi, P., Binzel, R.P. (Eds.), Asteroids III. Univ. of Arizona Press, Tucson, pp. 603–612.

Laskar, J., Robutel, P., 2001. High order symplectic integrators for perturbed Hamiltonian systems. Celest. Mech. Dynam. Astron. 80, 39–62.

La Spina, A., Paolicchi, P., Penco, U., 2005. Yarkovsky-evolved asteroid dynamical families: A correlation between their present properties and the impact geometry? Bull. Am. Astron. Soc. 37, 1514.

Lazzaro, D., Angelia, C.A., Carvanoa, J.M., Mothé-Diniz, T., Duffard, R., Florczak, M., 2004. S^3OS^2: The visible spectroscopic survey of 820 asteroids. Icarus 172, 179–220.

Levison, H., Duncan, M., 1994. The long-term dynamical behavior of short-period comets. Icarus 108, 18–36.

Love, S.G., Ahrens, T.J., 1996. Catastrophic impacts on gravity dominated asteroids. Icarus 124, 141–155.

Marzari, F., Cellino, A., Davis, D.R., Farinella, P., Zappalà, V., Vanzani, V., 1996. Origin and evolution of the Vesta asteroid family. Astron. Astrophys. 316, 248–262.

Milani, A., Knežević, Z., 1990. Secular perturbation theory and computation of asteroid proper elements. Celest. Mech. Dynam. Astron. 49, 347–411.

Milani, A., Knežević, Z., 1992. Asteroid proper elements and secular resonances. Icarus 98, 211–232.

Milani, A., Knežević, Z., 1994. Asteroid proper elements and the dynamical structure of the asteroid main belt. Icarus 107, 219–254.

Morbidelli, A., 2002. Modern Celestial Mechanics: Aspects of Solar System Dynamics. Taylor & Francis, London.

Morbidelli, A., Nesvorný, D., 1999. Numerous weak resonances drive asteroids toward terrestrial planets orbits. Icarus 139, 295–308.

Morbidelli, A., Nesvorný, D., Bottke, W.F., Michel, P., Vokrouhlický, D., Tanga, P., 2003. The shallow magnitude distribution of asteroid families. Icarus 162, 328–336.

Mothé-Diniz, T., Roig, F., Carvano, J.M., 2005. Reanalysis of asteroid families structure through visible spectroscopy. Icarus 174, 54–80.

Nesvorný, D., Bottke, W.F., 2004. Detection of the Yarkovsky effect for main-belt asteroids. Icarus 170, 324–342.

Nesvorný, D., Morbidelli, A., 1998. Three-body mean motion resonances and the chaotic structure of the asteroid belt. Astron. J. 116, 3029–3037.

Nesvorný, D., Bottke, W.F., Dones, L., Levison, H.F., 2002. The recent breakup of an asteroid in the main-belt region. Nature 417, 720–722.

Nesvorný, D., Bottke, W.F., Levison, H.F., Dones, L., 2003. Recent origin of the Solar System dust bands. Astrophys. J. 591, 486–497.

Nesvorný, D., Jedicke, R., Whiteley, R.J., Ivezić, Ž., 2005a. Evidence for asteroid space weathering from the Sloan Digital Sky Survey. Icarus 173, 132–152.

Nesvorný, D., Enke, B.L., Bottke, W.F., Durda, D.D., Asphaug, E., Richardson, D.C., 2005b. Karin cluster formation via asteroid impact. Icarus. In press.

Petit, J.-M., Farinella, P., 1993. Modeling the outcomes of high-velocity impacts between small Solar System bodies. Celest. Mech. Dynam. Astron. 57, 1–28.

Press, V.H., Teukolsky, S.A., Vetterlink, W.T., Flannery, B.P., 2001. Numerical Recipes in Fortran 77. Cambridge Univ. Press, Cambridge.

Rubincam, D.P., 2000. Radiative spin-up and spin-down of small asteroids. Icarus 148, 2–11.

Ryan, E.V., Melosh, H.J., 1998. Impact fragmentation: From the laboratory to asteroids. Icarus 133, 1–24.

Šidlichovský, M., Nesvorný, D., 1997. Frequency modified Fourier transform and its applications to asteroids. Celest. Mech. Dynam. Astron. 65, 137–148.

Sunshine, J.M., Bus, S.J., McCoy, T.J., Burbine, T.H., Corrigan, C.M., Binzel, R.P., 2004. High-calcium pyroxene as an indicator of igneous differentiation in asteroids and meteorites. Meteorit. Planet. Sci. 39, 1343–1357.

Sykes, M.V., 1988. IRAS observations of extended zodiacal structures. Astrophys. J. 334, L55–L58.

Tedesco, E.F., Noah, P.V., Noah, M., Price, S.D., 2002. The supplemental IRAS minor planet survey. Astron. J. 123, 1056–1085.

Vokrouhlický, D., 1998. Diurnal Yarkovsky effect as a source of mobility of meter-sized asteroidal fragments. I. Linear theory. Astron. Astrophys. 335, 1093–1100.

Vokrouhlický, D., 1999. A complete linear model for the Yarkovsky thermal force on spherical asteroid fragments. Astron. Astrophys. 344, 362–366.

Vokrouhlický, D., Brož, M., 2002. Interaction of the Yarkovsky-drifting orbits with weak resonances: Numerical evidence and challenges. In: Celletti, A., Ferraz-Mello, S., Henrard, J. (Eds.), Modern Celestial Mechanics: From Theory to Applications. Kluwer Academic, Dordrecht, pp. 467–472.

Vokrouhlický, D., Čapek, D., 2002. YORP-induced long-term evolution of the spin state of small asteroids and meteoroids. Rubincam's approximation. Icarus 159, 449–467.

Vokrouhlický, D., Farinella, P., 1999. The Yarkovsky seasonal effect on asteroidal fragments: A nonlinearized theory for spherical bodies. Astron. J. 118, 3049–3060.

Vokrouhlický, D., Brož, M., Morbidelli, A., Bottke, W.F., Nesvorný, D., Lazzaro, D., Rivkin, A.S., 2002. Yarkovsky footprints in the Eos family. Presented at the Asteroids, Comets and Meteors Meeting, Berlin. Abstract No. 12.01.

Vokrouhlický, D., Brož, M., Morbidelli, A., Bottke, W.F., Nesvorný, D., Lazzaro, D., Rivkin, A.S., 2006a. Yarkovsky footprints in the Eos family. Icarus. In press.

Vokrouhlický, D., Brož, M., Bottke, W.F., Nesvorný, D., Morbidelli, A., 2006b. Yarkovsky/YORP chronology of asteroid families. Icarus. In press.

Zappalà, V., Cellino, A., Farinella, P., Knežević, Z., 1990. Asteroid families. I. Identification by hierarchical clustering and reliability assessment. Astron. J. 100, 2030–2046.

Zappalà, V., Bendjoya, P., Cellino, A., Farinella, P., Froeschlé, C., 1995. Asteroid families: Search of a 12,487-asteroid sample using two different clustering techniques. Icarus 116, 291–314.